nature electronics

SUPPLEMENTARY INFORMATION

https://doi.org/10.1038/s41928-020-0416-x

In the format provided by the authors and unedited.

Analogue switches made from boron nitride monolayers for application in 5G and terahertz communication systems

Myungsoo Kim[1], Emiliano Pallecchi[2], Ruijing Ge[1], Xiaohan Wu[1], Guillaume Ducournau[2], Jack C. Lee[1], Henri Happy[2] and Deji Akinwande[1]✉

[1]Microelectronics Research Center, The University of Texas, Austin, TX, USA. [2]IEMN, University of Lille, CNRS UMR8520, Villeneuve d'Ascq, France.
✉e-mail: deji@ece.utexas.edu

Analogue Switches made from Boron Nitride Monolayers for Application in 5G and Terahertz Communication Systems

Myungsoo Kim[†], Emiliano Pallecchi[‡], Ruijing Ge[†], Xiaohan Wu[†], Guillaume Ducournau[‡], Jack C. Lee[†], Henri Happy[‡] and Deji Akinwande*[,†]

[†]Microelectronics Research Center, The University of Texas at Austin, Texas 78758, United States

[‡]IEMN, University of Lille, CNRS UMR8520, Avenue Poincaré, CS-60069, 59652 Villeneuve d'Ascq, France
[*]Corresponding Author: Deji Akinwande (deji@ece.utexas.edu)

Supplementary Figures

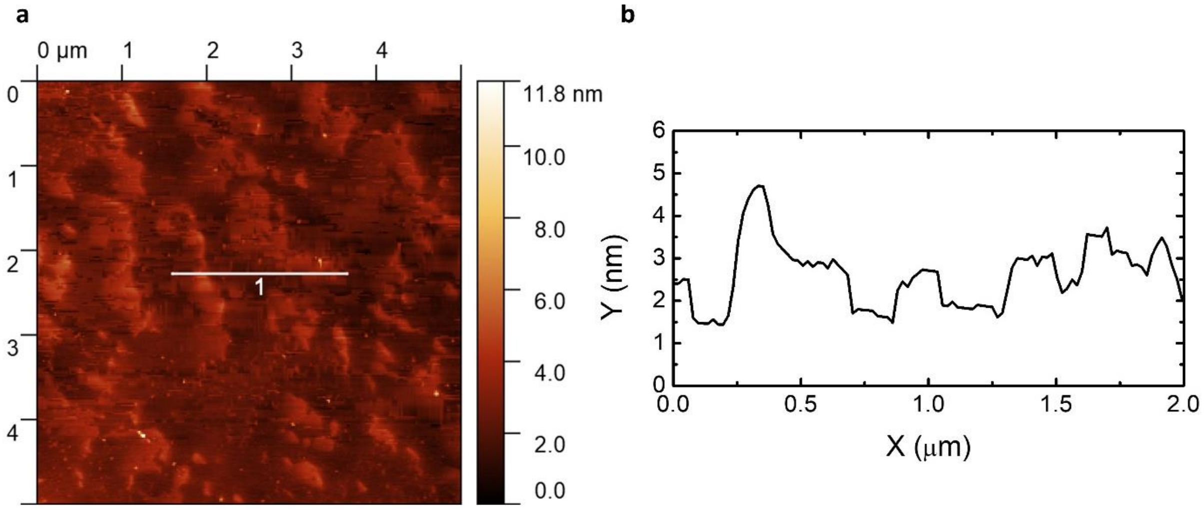

Supplementary Figure 1| Surface roughness of the CVD diamond substrate (a) Surface topography of the CVD diamond substrate. RMS (root mean square) roughness is less than 0.8 nm for 5 × 5 µm area. (b) Extracted profile along line 1 from (a).

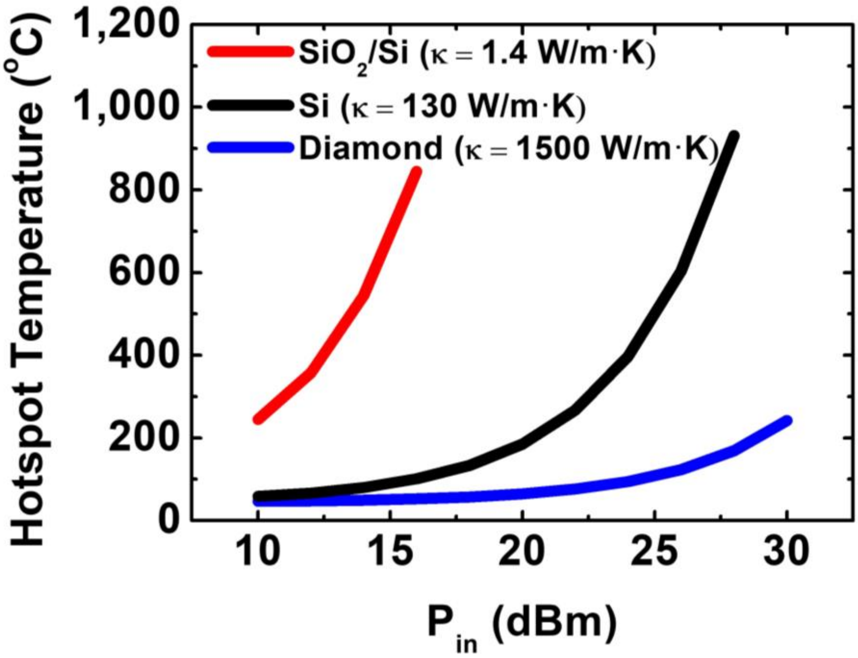

Supplementary Fig. 2| Heat sinking performance of different substrates The figure shows the simulated hotspot temperature of the switch device on SiO_2/Si, Si, diamond substrates. SiO_2/Si substrate have a 300 nm SiO_2 and bulk Si stack. This simulation shows that diamond is a superior substrate for heat sinking owing to its much higher thermal conductivity, κ.

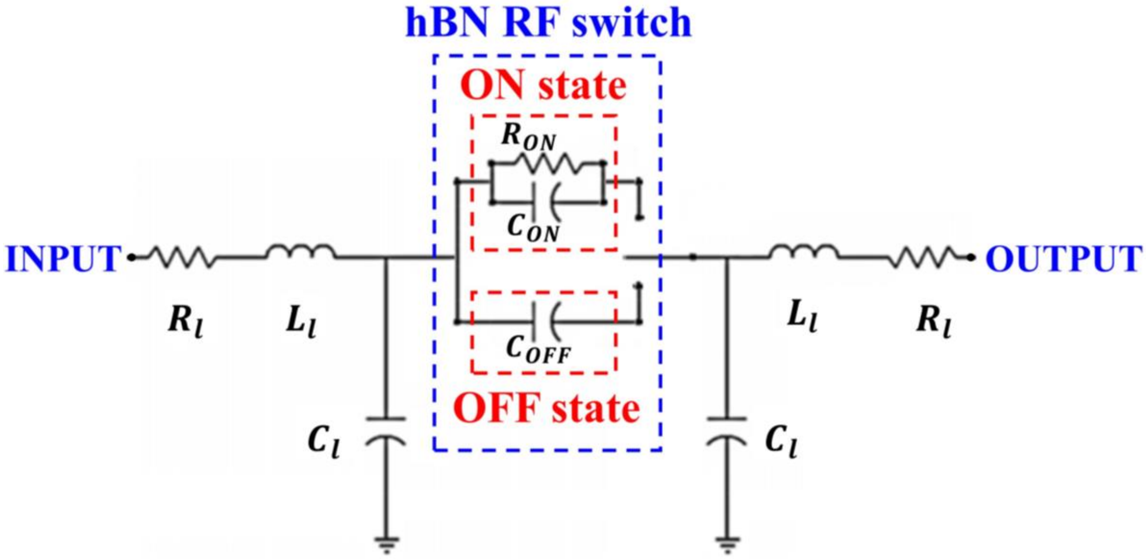

Supplementary Fig. 3| Lumped element equivalent circuit model The figure shows the equivalent hBN RF switch circuit model. The model includes the characteristic impedance, Z_0 at input and output terminals; a line resistor, R_l; a line inductor, L_l; a shunt coupling capacitor to ground, C_l; a switch OFF-state capacitor, C_{OFF} or an ON-state resistance, R_{ON} and ON-state capacitor, C_{ON} . The *RLC* line components in the model are the interconnect parasitics which are de-embedded with on-chip THRU and OPEN devices.

Supplementary Notes

Supplementary Note 1. Equivalent lumped element circuit model and S-parameter equation

As reported by the T-equivalent circuit model, S_{21} of the circuit from the Supplementary Fig. 2 is given by

$$S_{21} = \frac{2}{2 + (Z_0 + Z_2 + Z_2)/Z_3 + (Z_1 + Z_2 + \frac{Z_1 Z_2}{Z_3})/Z_0} \tag{1}$$

where

$$Z_1 = R_l + j\omega L_l \tag{2}$$

$$Z_2 = \begin{cases} 1/j\omega C_{\mathrm{OFF}} \\ R_{\mathrm{ON}} \end{cases} \tag{3}$$

$$Z_3 = \frac{1}{j\omega C_l} \tag{4}$$

ω is the angular frequency.

The switch capacitance, C_{OFF}, is an important factor that affects the isolation of the switch in the OFF-state of the switch. In order to de-embed the the effects of the line resistor, R_l, the scattering parameters of the same device structure without 2D material (Thru) are measured and de-embedded it from the ON-state measurement.

OFF-state isolation and ON-state insertion loss can be simplified as

$$S_{21,\,\mathrm{Isolation}} \approx \frac{2}{2 + (\frac{1}{j\omega C_{\mathrm{OFF}}})/Z_0} \tag{5}$$

$$S_{21,\,\mathrm{Loss}} \approx \frac{2}{2 + R_{ON}/Z_0} \tag{6}$$

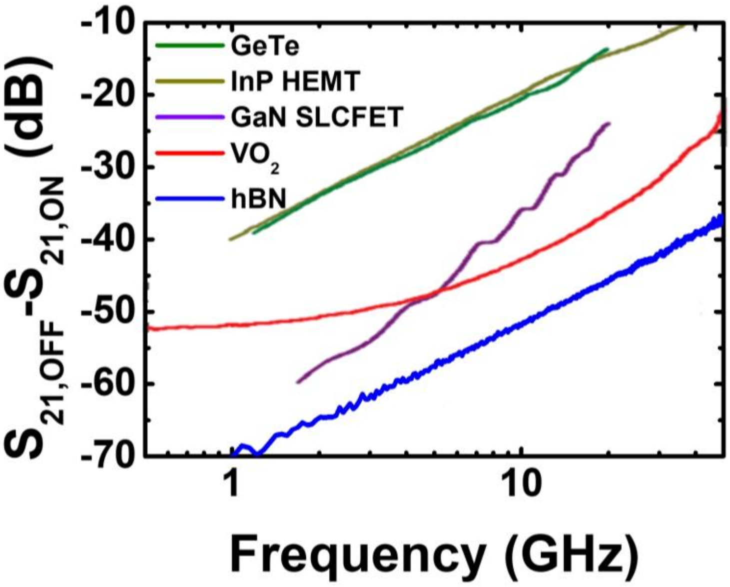

Supplementary Fig. 4| Comparison of $S_{21,OFF}$ - $S_{21,ON}$ ratios for different RF switch technology

Comparison of $S_{21,OFF}$ - $S_{21,ON}$ ratios for monolayer hBN RF switch in this work with GeTe[1], InP HEMT (High Electron Mobility Transistor)[2], GaN SLCFET (Super-Lattice Castellated Field Effect Transistor)[3], and VO_2 RF switch[4] from published literature. This figure highlights the superior performance of hBN switch to other device switches. For example at 50 GHz, hBN switch affords a switching ratio improvement of ≥ 10 dB compared to the VO_2 or other RF switches.

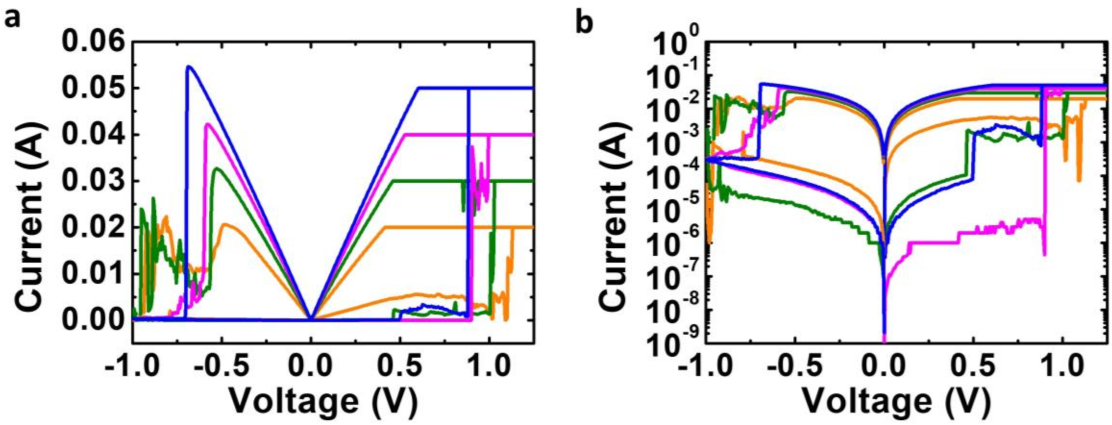

Supplementary Fig. 5| I-V curves of monolayer hBN switches with different compliance current

(a,b) Typical I-V curves of bipolar resistive switching behavior in monolayer hBN MIM device in linear and log scale. DC cycling measurements are conducted with 20, 30, 40, and 50 mA compliance currents. The monolayer hBN device has an overlap area of $0.5 \times 0.5\ \mu m^2$.

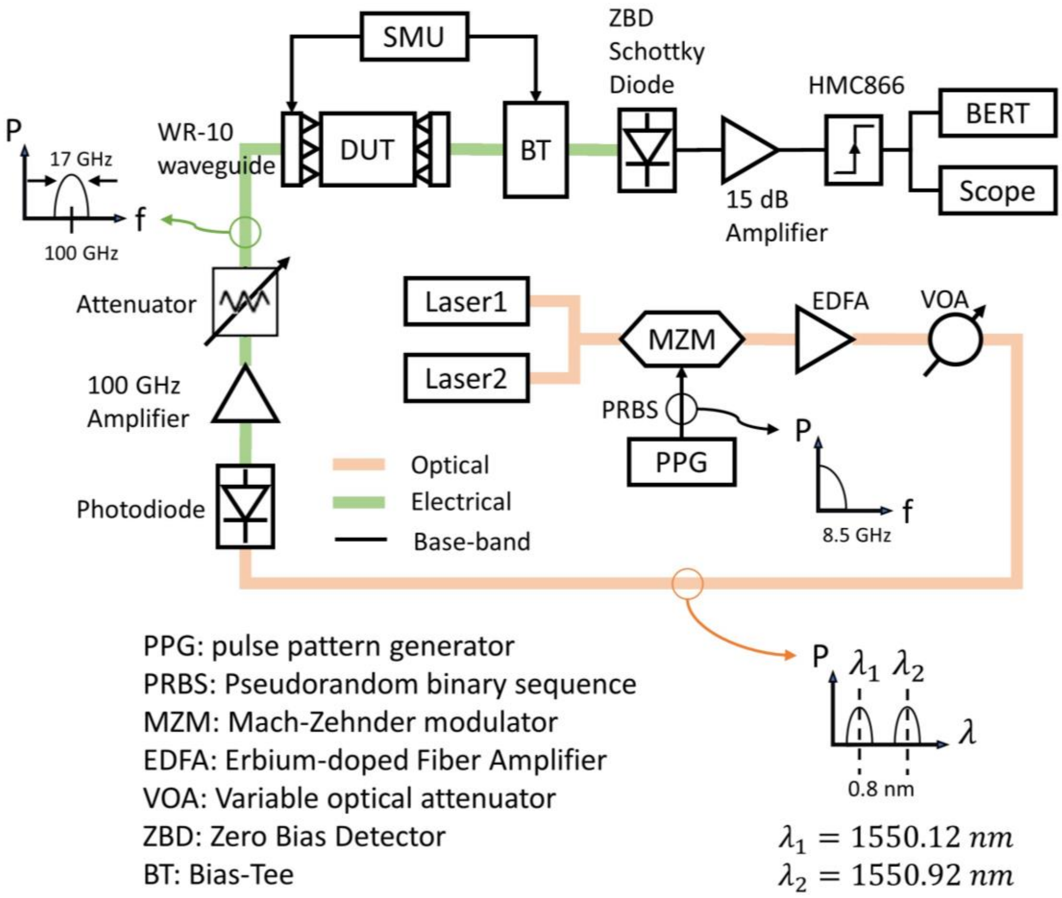

Supplementary Fig. 6| Eye-diagram and BER measurement setup The detailed experimental setup for eye-diagram and BER measurements use the photomixing of optical waves. Two 1550 nm lasers, separated by 0.8 nm (this separation corresponds to 100 GHz) are amplitude modulated using a Mach-Zehnder Modulator (MZM) and a pseudo-random bit sequence (PRBS) with a 2^9-1 length. The modulated optical signals are used to feed a 100 GHz photodiode which generates a modulated 100 GHz electrical signal, thanks to the photomixing down-conversion inside the Photodetector. This 100 GHz signal is then amplified and a variable attenuator is used to accurately control the power level at the device under test (DUT) input port (coplanar access at wafer level). After the propagation across the device, the 100 GHz signal is detected by a Schottky barrier diode, used as an envelope detector. After this detector, the signal is amplified using a 15 dB amplifier which drive a buffer amplifier (Hittite HMC866) required to drive the bit error rate tester (BERT). We used data-rate up to 8.5 Gbit/s and The measurements were conducted over the frequency range of the modulated signal: 91.5-108.5 GHz (± 8.5 GHz around the 100 GHz carrier).

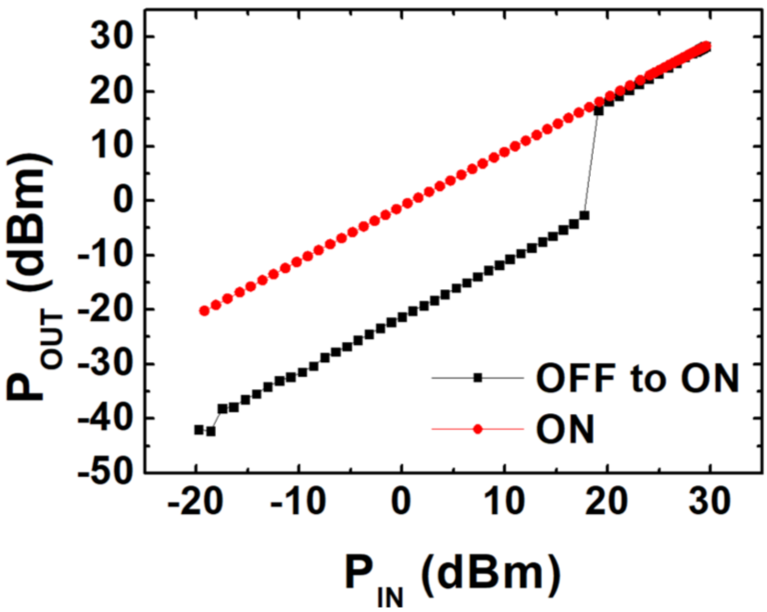

Supplementary Fig. 7| Output RF power vs. Input RF power at 40 GHz input signal Power handling measurement for 40 GHz signal at the same device. The device was at OFF-state then the input power was ramped up. Around 20 dBm, the device experienced self-switching. After input RF power reached 30 dBm, the device was measured again from -20 dBm input power. From 20 dBm to 30 dBm input power, the first and second measurements show a similar trend.

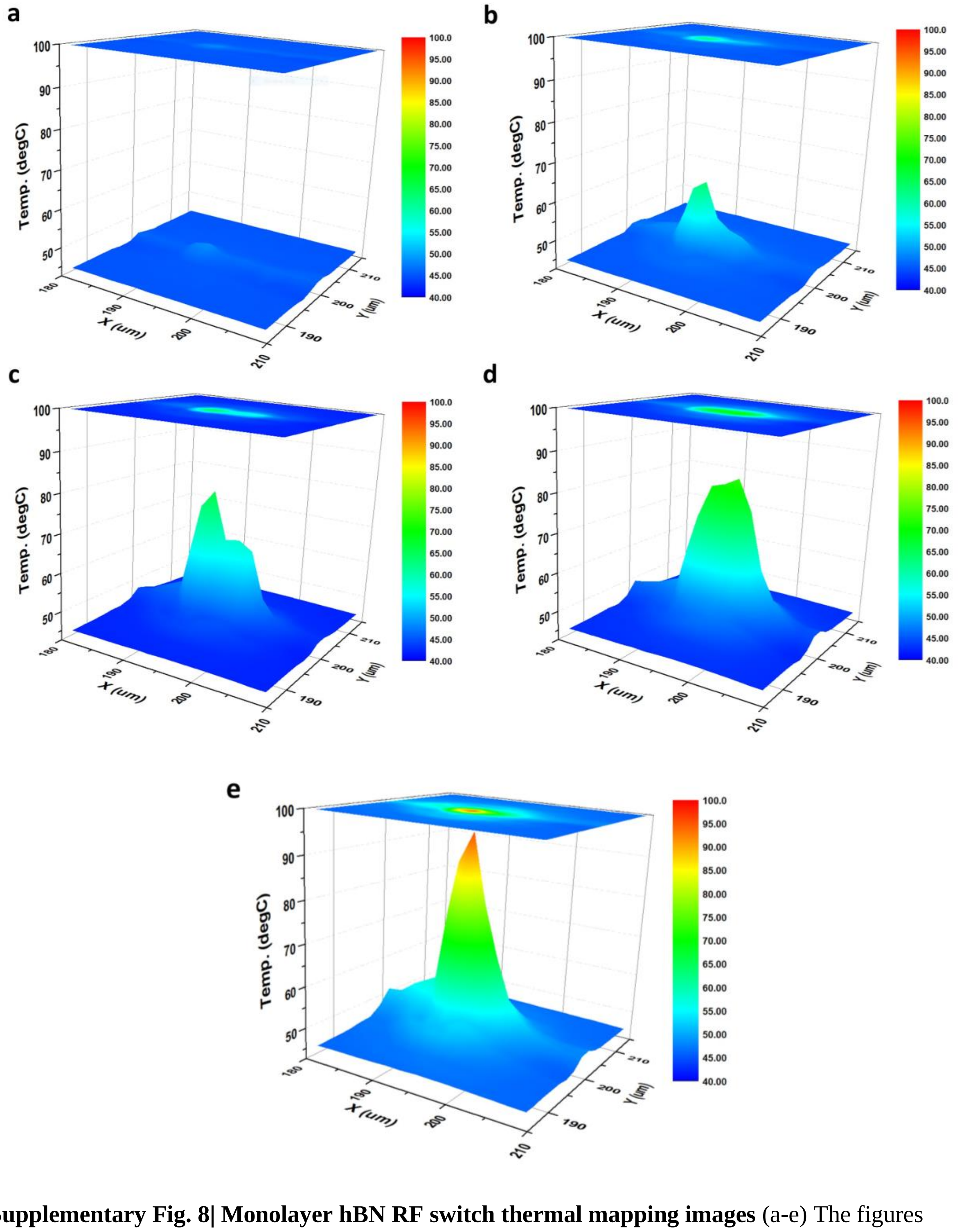

Supplementary Fig. 8| Monolayer hBN RF switch thermal mapping images (a-e) The figures represent thermal mapping images of the device junction area at 19.7 dBm, 23 dBm, 25.5 dBm, 28 dBm, 29.3 dBm from (a) to (e). Temperature data was measured with a pixel resolution of 2 × 2 μm^2.

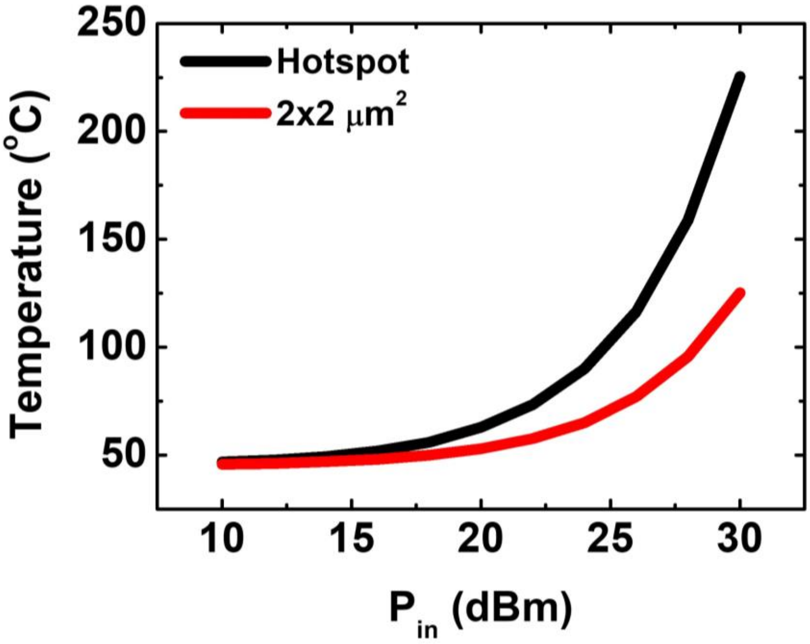

Supplementary Fig. 9| COMSOL Thermal simulation of the experimental mesa structure

Temperature dependence on the input power at device overlap area. The maximum hotspot and averaged (2×2 μm^2 area) temperatures are shown for comparison. The averaged temperature allows for comparison with experimental thermal mapping data, and the hotspot temperature provides insight into the local peak temperature of the device.

Supplementary Tables

Supplementary Table 1. hBN RF switch comparison table

Device Technology	Non-volatility	Control Voltage	Cutoff frequency	Operating Environment	Switching time	Dimension (single device W x L)	Max Power (dBm)
hBN Switch (This Work)	**Yes**	**~1 - 3V**	**129 THz**	**Ambient condition**	**< 15 ns**	**0.2 μm x 0.15 μm**	**20**
MoS_2 Switch[5]	Yes	~0.5 – 1.5V	70 THz	Ambient condition	< 15 ns	0.15 μm x 0.2 μm	10
GeTe Phase-change Switch[6]	Yes	1.1 V	21 THz	Heater needed	~120 ns	19 μm x 1 μm	27
Memristive switch[7]	Yes	3V	35.2 THz	Ambient condition	Not reported	0.11 μm x 0.035 μm	17
VO_2 Phase-change Switch[8]	No	~2 V	45 THz	Heater needed	2 us	2 μm x 10 μm	17
MEMS Switch[9]	No	80~90 V	12.4 THz	Hermetic packaging	~5 us	250 μm x 250 μm	>25

Supplementary Note 2. Live HD-TV stream demonstration

The data stream recorded with a commercial HD-TV camcorder is used uncompressed to modulate a carrier at 100 GHz, sent through the hBN switch, demodulated and fed to a standard TV screen. The HD-TV stream was performed with the setup for BER measurements, with the HD-TV data stream from the camcorder replacing the PRBS signal. A video of the demonstration is available as a 'Supplementary Video File' on the journal website.

At the beginning of the video, the HD-TV data at 100 GHz are sent through a device in the ON state. The eye pattern is clearly visible and, owing to the low BER, the HD-TV live stream appears on the TV. Then, the hBN switch is RESET using a DC pulse: the HD-TV transmission vanishes and the eye pattern closes.

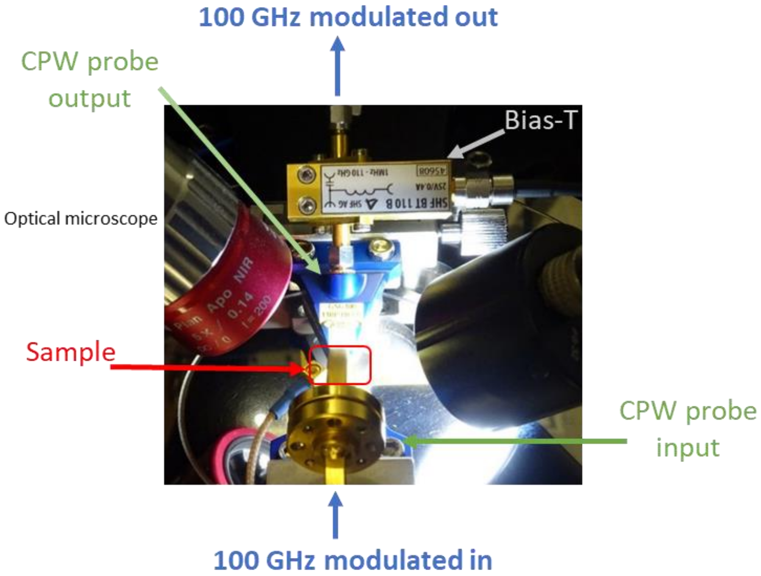

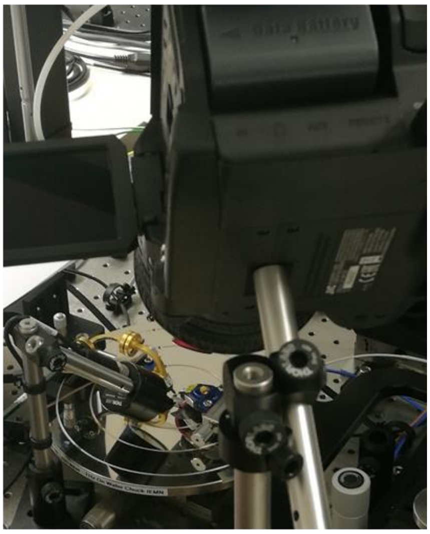

HD-TV stream (left) Image of the setup used during the HD-TV live demo. The device is connected with two coplanar probes for 100 GHz modulated input and output, the DC signal used for SET/RESET process of the switch is added via bias-T. (right) Camcorder-setup used for recording the live HD-TV stream.

Supplementary References

1. El-Hinnawy N, *et al.* 12.5 THz Fco GeTe inline phase-change switch technology for reconfigurable RF and switching applications. In: *2014 IEEE Compound Semiconductor Integrated Circuit Symposium (CSICS)*). IEEE (2014).

2. Kamitsuna H, Yamane Y, Tokumitsu M, Sugahara H, Muraguchi M. Low-power InP-HEMT switch ICs integrating miniaturized 2/spl times/2 switches for 10-Gb/s systems. *IEEE journal of solid-state circuits* **41**, 452-460 (2006).

3. Howell RS, *et al.* Low loss, high performance 1-18 GHz SPDT based on the novel super-lattice castellated field effect transistor (SLCFET). In: *2014 IEEE Compound Semiconductor Integrated Circuit Symposium (CSICs)*). IEEE (2014).

4. Madan H, *et al.* 26.5 Terahertz electrically triggered RF switch on epitaxial VO2-on-Sapphire (VOS) wafer. In: *2015 IEEE International Electron Devices Meeting (IEDM)*). IEEE (2015).

5. Ge R, *et al.* Atomristors: Memory Effect in Atomically-thin Sheets and Record RF Switches. In: *2018 IEEE International Electron Devices Meeting (IEDM)*). IEEE (2018).

6. Léon A, *et al.* RF Power-Handling Performance for Direct Actuation of Germanium Telluride Switches. *IEEE Transactions on Microwave Theory and Techniques*, (2019).

7. Pi S, Ghadiri-Sadrabadi M, Bardin JC, Xia Q. Nanoscale memristive radiofrequency switches. *Nature Communications* **6**, 7519 (2015).

8. Field M, Hillman C, Stupar P, Hacker J, Griffith Z, Lee K-J. Vanadium dioxide phase change switches. In: *Open Architecture/Open Business Model Net-Centric Systems and Defense Transformation 2015*). International Society for Optics and Photonics (2015).

9. Patel CD, Rebeiz GM. A compact RF MEMS metal-contact switch and switching networks. *IEEE Microwave and Wireless Components Letters* **22**, 642-644 (2012).